

# EFFICIENCY IMPROVEMENT OF VERTICAL-AXIS WIND TURBINES WITH COUNTER-ROTATING LAY-OUT

**Nicolas Parneix, Rosalie Fuchs, Alexandre Immas, Frédéric Silvert**

NENUPHAR, Campus de l'Institut Pasteur, 1 rue du Professeur Calmette, 59000 Lille, France

**Paul Deglaire**

ADWEN, 60 Avenue du Général de Gaulle, 92800 Puteaux

## 1 Abstract

, This paper demonstrates the effect of a counter-rotating lay-out of two high power vertical axis wind turbines to improve the power efficiency of each vertical axis wind turbine.

Numerical modelling is carried out to evaluate the parameters that have the greatest influence on the increase in power with two counter-rotating wind turbines. The calculations are performed with CFD and an in-house code based on vortex methods.

The contraction of the flow between both wind turbines induces a Power coefficient ( $C_p$ ) increase of up to 15% at a rotor axis inter-distance of 1.2D for 2D simulations, and at least 8% for 3D simulations.

## 2 Keywords

VAWT, Vertical Axis Wind Turbines, Floater, Counter-rotating, Numerical simulations, CFD, Vortex model, Streamtubes contractions

## 3 Introduction

Improving the performance of Vertical Axis Wind Turbines (VAWTs) is key to make VAWTs commercially successful. Scientists have investigated several interesting concepts for that purpose: increasing the swept area, especially to limit the losses due to 3D effects, or using flap and pitch systems to control the flow around the blades [1, 2].

NENUPHAR, with the TWINFLOAT® concept (see Figure 1), propose to take advantage of all these concepts combined with an aerodynamic effect called the counter-rotating effect [3]. The TWINFLOAT® concept is made of two 2.5MW VAWT on one single floater, to reach a total rated power of 5MW. The proximity of the two rotors generates a contraction of the streamtubes that flow in the area between the rotors, thus increasing the air flow rate going through both the rotors' swept areas and thereby the performance of each VAWT.

This concept has also other advantages: smaller rotors components and drivetrains that make easier their fabrication, their installation and Operating and Maintenance (O&M) operations, floater motions reduction thanks to specific control laws and wake reduction leading to an increase in the capacity factor of a TWINFLOAT® wind farm.

Simulations presented in this paper are carried out by Computational Fluid Dynamics (CFD) calculations or by using a Vortex Panel Method to investigate the streamtubes contraction caused by counter-rotating wind turbines and the impact of the distance between each rotor.

This paper presents the main results of this study and the positive impact of counter rotating turbines compared to single turbine performance for floating conditions.



**Figure 1: The TWINFLOAT® concept (© Nenuphar)**

## 4 Model, material and methods

Modelling the TWINFLOAT® concept (see Figure 1), simulations are carried out to investigate the physical flow around one or two wind turbines, with various distances between the two wind turbines axes.

To study the benefits of the counter-rotating concept compared to one isolated VAWT, a vortex code (ARDEMA) has been developed by ADWEN OFFSHORE and NENUPHAR. To get a better modelling of the viscous effects, a CFD (Computational Fluid Dynamics) modelling strategy has also been developed by NENUPHAR.

As the flow regime encountered by a typical VAWT is at relatively low speed (Mach number  $M < 0.3$ ) and a Reynolds number in the range  $10^5$  to  $10^7$ , both models consider incompressible flow.

The main difference between the two types of calculation is the modelling of the viscous effects: they are inherently calculated in CFD simulations but are calculated using a semi-empirical model in the vortex method code.

### 4.1 Vortex method ARDEMA combined with a Dynamic Stall model

#### 4.1.1 Inviscid solver

The multi-body vortex code ARDEMA [4, 5] solves the Euler equation (Eq. 2) that is the Navier-Stokes equations under the assumptions that the flow is incompressible, adiabatic and inviscid outside the boundary layer. In these conditions the mass conservation law reduces to Eq.1 and the velocity can be represented as the gradient of a scalar potential (potential flow) (Eq. 3) that satisfies the Laplace equation (Eq. 4).

$$\nabla \cdot q = 0 \quad (\text{Eq. 1})$$

$$\frac{\partial \vec{q}}{\partial t} + \vec{q} \cdot \nabla \vec{q} = \vec{f} - \frac{\nabla p}{\rho} \quad (\text{Eq. 2})$$

$$q = \nabla \Phi \quad (\text{Eq. 3})$$

$$\nabla^2 \Phi = 0 \quad (\text{Eq. 4})$$

The Laplace equation is a second order linear partial differential equation, so any linear combination of independent solutions (sources, doublets, vortices) is also a solution. The potential velocity solution is found using the Source Doublet formulation with Dirichlet Boundary conditions on the surface and Kutta conditions at the trailing edges.

From the potential velocity solution, the pressure is then computed using unsteady Bernoulli's equation, leading to the definition of the aerodynamic loads on the sections.

ARDEMA was validated against theoretical and experimental cases [4, 5], and is continuously improved and compared to experimental and numerical data coming from test campaigns performed both in wind tunnel and on NENUPHAR's real-scale onshore prototypes.

#### 4.1.2 Viscous correction

The inviscid ARDEMA solver was adapted to account for the dynamic stall phenomenon inherent to the complex aerodynamics involved in VAWT. A Beddoes-Leishman (BL) type dynamic stall model [6] [7] was implemented, extending the code validity domain to low TSR.

The BL model is coupled with ARDEMA, using the relative velocities and angle of attacks issued from the inviscid solver as model inputs. The BL model simulates flow separation, pressure lag and friction lag depending on empirical parameters to compute viscous corrected lift and drag variables.

#### 4.2 CFD

For this study, the CFD simulations are performed by implementing an incompressible flow regime with the commercial solver Ansys-Fluent V15, with a URANS (Unsteady Reynolds-Averaged Navier Stokes) method and closed with a SST (Shear Stress Transport)  $k-\omega$  Turbulence model. This model combines the capacity of the  $k-\omega$  model to model near wall turbulence in rotating flow, with the ability of the  $k-\omega$  model to model the free-stream turbulence [8].

CFD 2D simulations are carried out in a horizontal plane situated at the mid-height of the rotor (see Figure 2).

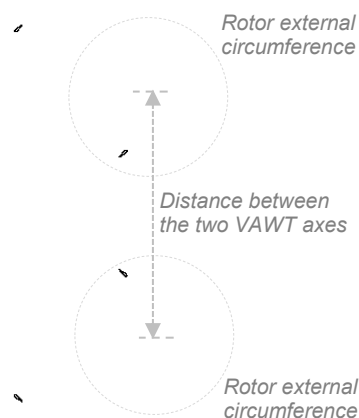


**Figure 2 : 2D model for simulations**

The spatial domain (i.e. numerical wind tunnel (NWT)) is decomposed into two distinct sub-domains:

- A rectangular outer zone, corresponding to the overall calculation domain, with circular openings centered on the wind turbines rotational axes.
- Circulars inner zones around each wind turbine.

The zones are separated with numerical interfaces.

Figure 3 presents the main dimensions and boundary conditions of the overall domain, whereas Figure 4 presents the blade azimuthal conventions for both wind turbines.

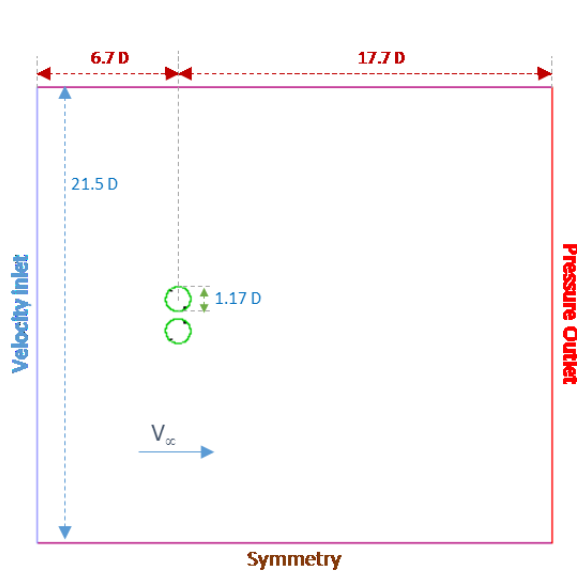


**Figure 3 : Main dimensions of the numerical wind tunnel**

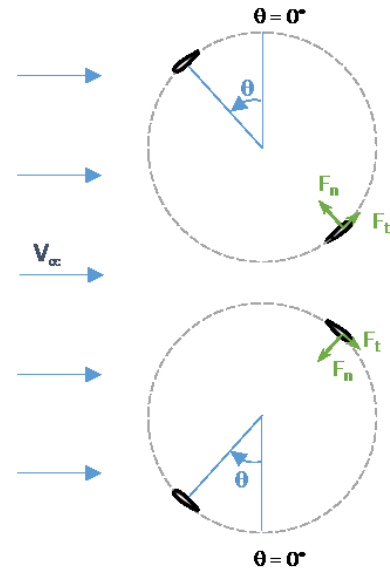


**Figure 4 : Blade azimuthal conventions**

The mesh is composed of prismatic mesh elements in the boundary layer areas of the blades to respect the numerical criteria of  $Y^+ = 1$ , with a growth factor of 1.25, and triangular mesh elements for the rest of the domain. Finally, the mesh is composed with  $1.062 \times 10^6$  elements. Figure 5 presents representations of the mesh.

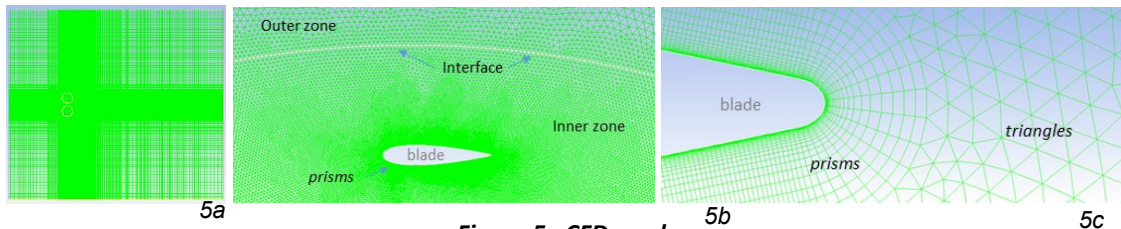


**Figure 5 : CFD mesh**

**(5a) is the global view of the NWT domain - (5b) is a zoom around a blade - (5c) is a zoom on the prism layer around the blade**

## 5 Results

### 5.1 Power gain depending on distance between the wind turbines axes (2D simulations)

The flow expansion resulting from the blockage effect of the wind turbines is reduced with two counter-rotating wind turbines because of a forced flow as it is showed on Figure 6.

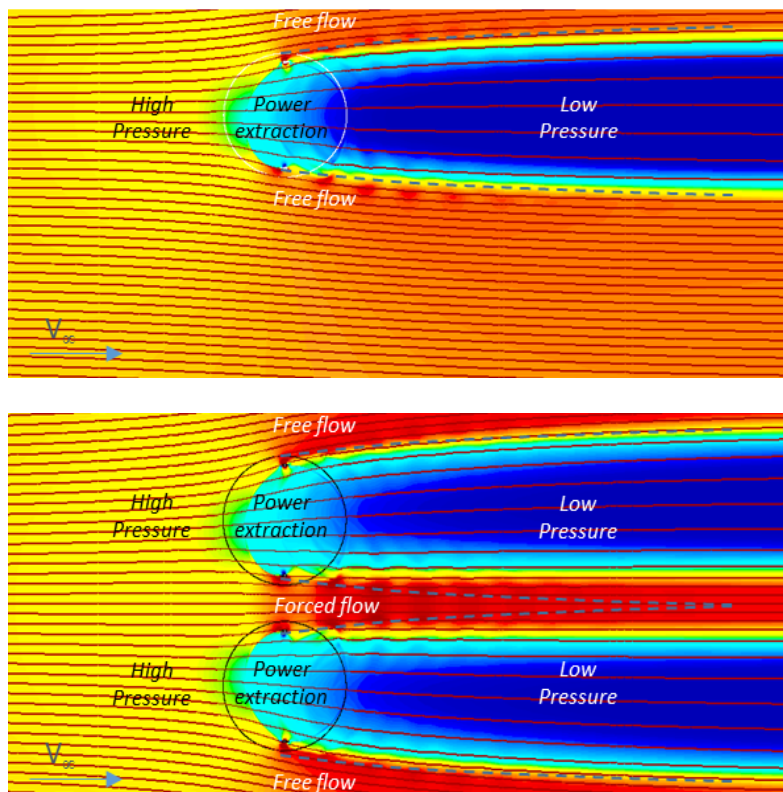


**Figure 6 : Forced flow with counter-rotating wind turbines (CFD simulations)**  
**Coloured by the non-dimensional velocity ( $V/V_\infty$ ), with streamlines**

Another effect of the forced flow between the two counter-rotating wind turbines is that each wind turbine extracts more energy from the wind (blue curve on Figure 8) than an isolated wind turbine (red curve on Figure 8).

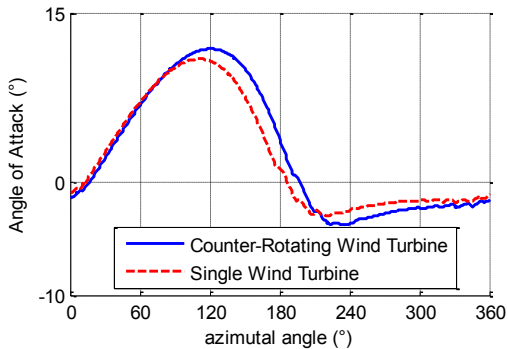


**Figure 7 : Angle of attack over one lap**

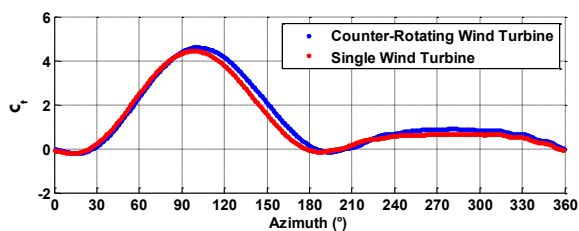


**Figure 8 : Normalized tangential forces**

Indeed, because of the forced flow, the air flow rate inside the rotor is increased, leading to a slight increase in the Angles of Attack (AoA) on the blades (see Figure 7). For the MPPT (Maximum Power Point Tracking) operating mode at maximum  $C_p$  conditions, as long as the wind turbines are rotating at a sufficiently high TSR, the AoA stays in the linear part of the lift curve. Hence, each increase in AoA leads to an increase in the Lift/Drag ratio, resulting to an increase in the normalized tangential force  $C_t$  (see Figure 8), and finally to an increase in the Power coefficient  $C_p$ .

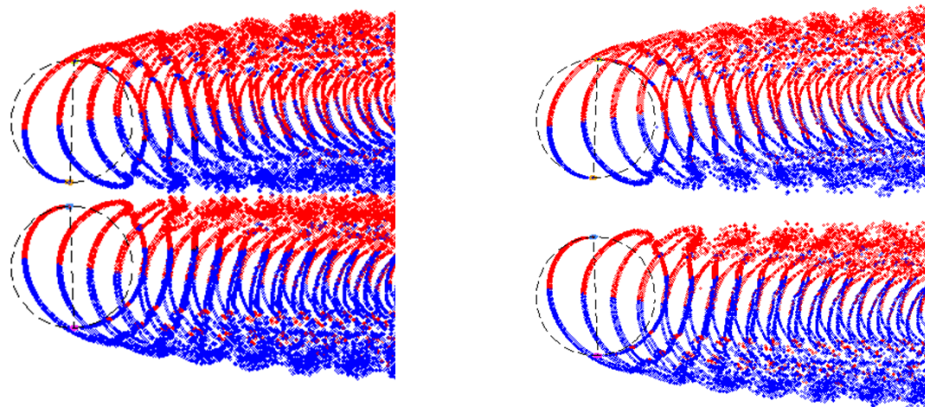


**Figure 9 : Wake of the counter-rotating VAWT with a distance of 1.2D and 1.5D at the same TSR=3.5 (ARDEMA simulations)**

Figure 9 presents the wake structure for two distances between the rotors in a counter-rotating lay-out. The inward and outward wake structures are dependent on this distance and the increase in power with the counter-rotating wind turbines is obviously dependent on the distance between both wind turbines, which is confirmed with the results presented on Figure 10

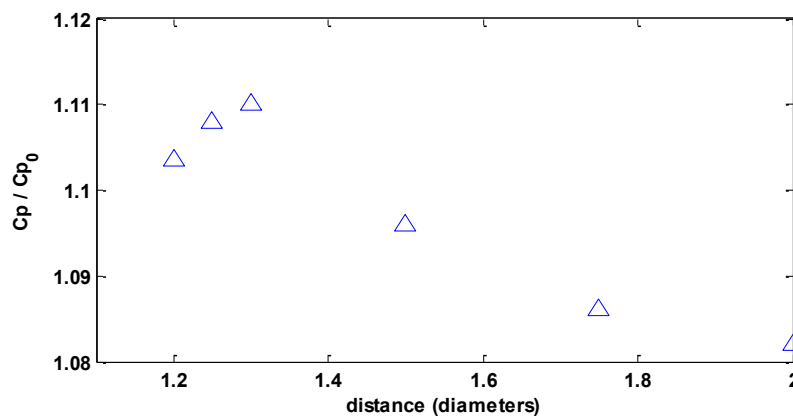


**Figure 10 : Performance vs. distance between the rotors' axes at iso-TSR**

## 5.2 Increase of TSR with counter-rotating wind turbines

The optimal TSR is also increased by up to 0.4 (10% higher) with counter-rotating wind turbines, which is aerodynamically interesting as long as the operating points are moved away from dynamic stall limits.

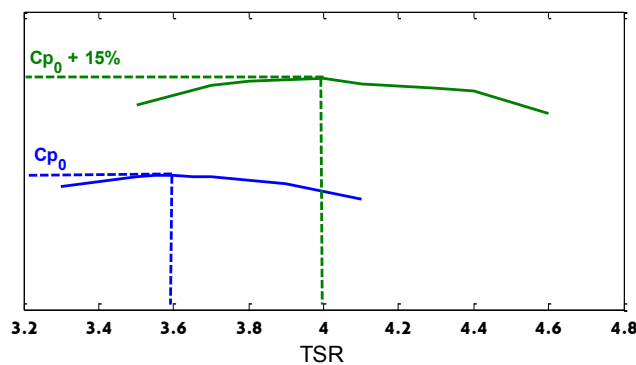


**Figure 11 : Cp vs. TSR curves for the single (blue) and counter-rotating (green) wind turbines**

### 5.3 Power gain depending on distance between the wind turbines axes (3D simulations)

Many other effects usually called “3D effects”, including blade tips losses and rotor aspect ratio, provide additional parameters that impact the results presented previously.

Figure 12 presents the relative variation of Cp resulting from 3D simulations carried out using ARDEMA [4, 5]. Calculation are performed at a constant TSR of 4.2 (which obviously does not permit to determine the maximum power increase but however allows to capture the efficiency trend), and for different distances between both rotor axes.

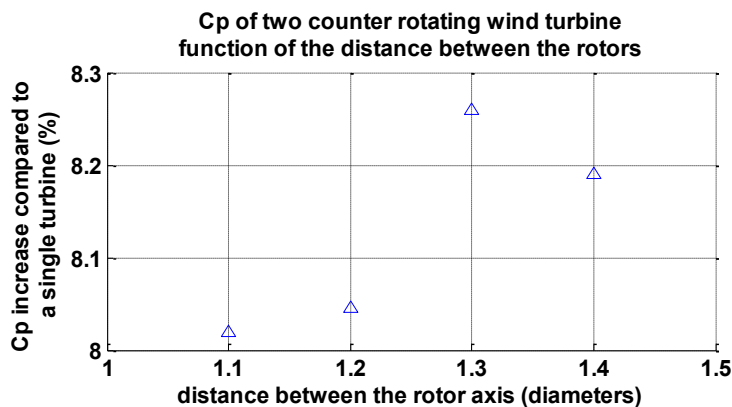


**Figure 12 : Performance vs. distance between the rotor axes at constant TSR in 3D**

The conclusions are similar to the ones of the previous paragraph obtained with 2D simulations:

- ⇒ the optimal distance is between 1.2 and 1.4 diameters,
- ⇒ the counter-rotating layout of vertical axis wind turbines induces a Cp increase. Due to 3D effects and the fact that the 3D simulations were run at constant TSR, the estimated gain calculated with 3D simulations (8%) is lower than the one calculated with 2D simulations (15%).

## 6 Conclusion

The paper presents numerical results of two counter-rotating wind turbines with a URANS formulation and with a vortex method. It shows that both numerical tools can realistically simulate the flow around counter-rotating VAWTs. A streamtubes contraction or forced flow effect is observed between the two wind turbines, which increases the mass flow rate that goes through the rotors' swept areas. A maximum Cp increase of up to 15% has been computed at a rotor axis inter-distance of 1.2D..

## 7 Learning objectives

These numerical results provide valuable information about how to increase the efficiency of VAWTs, thus improving confidence that the TWINFLOAT® concept can be designed with higher aerodynamic efficiency. This is a crucial step in order to make VAWTs competitive on the wind energy market.

The next step of this TWINFLOAT® counter-rotating technology development will include experimental tests in a wind tunnel to validate the numerical tools. The offshore deployment of the first TWINFLOAT® prototype by 2019 will also bring valuable measurements at large-scale

to confirm the performance increase that has already been numerically calculated or that is currently measured on reduced-scale rotors in wind tunnels.

## References

- [1] S. Ertem, *Enhancing the Features of Vertical Axis Wind Turbines with Active Flap Control and Airfoil Design*, Master of Sciences Thesis, Delft University of technology, 2015
- [2] B. Paillard, *Numerical simulation and optimization of a crossflow axis tidal turbine with active pitch control*, PhD thesis, 2011
- [3] J.O. Dabiri, *Potential order-of-magnitude enhancement of wind farm power density via counter-rotating vertical-axis wind turbine arrays*, J. Renew. Sust. Energy 3 (2011), 043104.
- [4] P Deglaire, *Analytical aerodynamic simulation tools for vertical axis wind turbines*, PhD thesis Uppsala University 2010
- [5] B.A.Sc, K. R. Dixon, *The near wake structure of a Vertical Axis Wind Turbine*, Delft University of Technology, Master of thesis, 2008
- [6] Leishman, J. G., and T. S. Beddoes, *A generalised model for airfoil unsteady aerodynamic behaviour and dynamic stall using the indicial method*, Proceedings of the 42nd Annual forum of the American Helicopter Society, Washington DC, 1986
- [7] Beaudet, Laurent, *Etude expérimentale et numérique du décrochage dynamique sur une éolienne à axe vertical de forte solidité*, Diss. Université de Poitiers, 2014 (French)
- [8] *Ansys Fluent Theory Guide*. Release 15.0, November 2013